COMMUNICATIONS

Quantification of Relative Cerebral Blood Flow Change by Flow-Sensitive Alternating Inversion Recovery (FAIR) Technique: Application to Functional Mapping

Seong-Gi Kim

Relative cerebral blood flow changes can be measured by a novel simple blood flow measurement technique with endogenous water protons as a tracer based on flow-sensitive alternating inversion recovery (FAIR). Two inversion recovery (IR) images are acquired by interleaving slice-selective inversion and nonselective inversion. During the inversion delay time after slice-selective inversion, fully magnetized blood spins move into the imaging slice and exchange with tissue water. The signal enhancement (FAIR image) measured by the signal difference between two images is directly related to blood flow. For functional MR imaging studies, two IR images are alternatively and repeatedly acquired during control and task periods. Relative signal changes in the FAIR images during the task periods represent the relative regional cerebral blood flow changes. The FAIR technique has been successfully applied to functional brain mapping studies in humans during finger opposition movements. The technique is capable of generating microvascular-based functional maps.

Key words: cerebral blood flow; perfusion; functional magnetic resonance imaging; functional brain mapping.

INTRODUCTION

Regional cerebral blood flow (rCBF) increases induced by neuronal activity have been the basis of several functional imaging techniques currently in use with humans, including positron emission tomography (PET) and single photon emission tomography (SPECT) (1). In contrast, the most widely used functional magnetic resonance imaging (fMRI) technique is based on blood oxygenation level-dependent (BOLD) effect (2–4), which is sensitive to alterations in local deoxyhemoglobin content (5–8). It is thought that neuronal activation within the cerebral cortex leads to an increase of rCBF without a commensurate elevation in oxygen consumption rate (9), which in turn causes a decrease in capillary and venous deoxyhemoglobin concentrations and hence increases in T_2*/T_2-weighted MR signal and BOLD contrast. This MR technique is sensitive enough to generate a functional map without intersubject or intrasubject averaging and has been successfully applied to functionally map the human brain during motor, vision, language, and cognition processes (e.g. (2–4) and (10–21)). BOLD-based functional imaging represents a clear breakthrough in our ability to examine aspects of brain function. However, the approach has some shortcomings, namely, (i) it is dependent on the presence of *uncoupling* between blood flow and oxygen consumption rate during increased neuronal activity which may not be present under all circumstances and in all regions of the brain (22–23), and (ii) quantification is at present virtually impossible due to the dependence on multiple parameters, such as absolute blood volume, blood volume and flow changes, and vessel size (24–26).

Alternative MR imaging (MRI)-based approaches are the methods that respond only to rCBF and/or cerebral blood volume (CBV) increases associated with a mental task irrespective of the consequences of increased neuronal activity on oxygen consumption rate. Initially, relative CBV was measured using an exogenous contrast agent during visual stimulation (27). However, the use of this technique is severely limited because of the need for repeated bolus injections of an exogenous contrast agent, and the necessity to compare images acquired during two different administrations of the contrast agent bolus separated by a relatively long period (several minutes). A slice-selective inversion recovery (IR)-based functional imaging technique which does not utilize exogenous agents has also been used to map visual stimulation in the brain (3). However, signal changes were relatively small and the method does not have the potential for measurements of relative flow changes, although it can determine the magnitude of the change in flow; the former is more informative for functional imaging studies. Furthermore, activation based on the IR technique has confounding effects from BOLD because of the inevitable T_2* weighting present in echo-planar imaging (EPI) images. It has been reported as abstracts that perfusion can be, in principle, determined from slice-selective and nonselective IR images (28-29). However, this technique has not been applied to measuring neuronal activity induced relative blood flow changes and generation of functional maps. Recently Edelman *et al.* (30) have reported a flow technique based on EPI and signal targeting with alternating radio frequency (EPISTAR), in which two images are acquired with and without spin tagging at the proximal end of the arterial blood and then sub-

MRM 34:293–301 (1995)

From the Center for Magnetic Resonance Research, Department of Radiology, University of Minnesota Medical School, Minneapolis, Minnesota.

Address correspondence to: Seong-Gi Kim, CMRR, University of Minnesota Medical School, 385 East River Road, Minneapolis, MN 55455.

This work was supported by National Institutes of Health Grants RR08079 and NS32919.

Received February 6, 1995; revised May 11, 1995; accepted May 12, 1995.

0740-3194/95 $3.00

tracted from each other. The tagged inversion pulse is applied to the inferior area of the slice of interest which has an axial orientation. They reported *ca.* 59% focal signal changes during motor and visual tasks (30). Although the signal changes in this approach are related to CBF alterations, the exact relationship between percent signal changes in the images and alterations in blood flow is not known (30). This technique is sensitive to T_1 of blood because, subsequent to spin "tagging" (i.e., inversion) below the axial slice of interest, the "tag" is lost by T_1 relaxation while spins travel into the imaging slice. Also, an inversion pulse in only one of the paired images is used (30), and thus the side lobe of the inversion pulse disturbs spins at the inferior side of the imaging slice; to eliminate this problem, slice-selective saturation pulses in both images are used.

To overcome the aforementioned problems, we demonstrate that perfusion-based functional images can be generated by subtracting two IR images, one with a non-slice-selective inversion pulse and another with a slice-selective inversion pulse. We call this technique flow-sensitive alternating inversion recovery (FAIR). The signal changes are directly correlated to CBF changes so that quantification of relative rCBF (relCBF) changes during mental processes is possible. Unlike EPISTAR, the tagged spin in the selective IR image is the unperturbed longitudinal magnetization (M_o) along the $+z$ direction outside the slice, and thus independent of the T_1 relaxation of blood water proton. Also, the same inversion pulse is applied in both IR images and thus any additional saturation pulses are not needed. FAIR also differs from the previously used simple IR-based functional imaging approach (3) because signal intensity is always compared between two acquisitions, one with slice-selective inversion where relaxation within the inverted slice is sensitive to flow and the other with global inversion where flow sensitivity is eliminated.

THEORY

Two IR images are acquired; one with a non-slice-selective inversion pulse and the other with a slice-selective inversion pulse. It is assumed in the following analyses that a repetition time (TR) is long enough to completely relax blood and tissue water spins. The longitudinal magnetization after a nonselective inversion pulse M_{ns} is $M_{ns}(t) = A - B\cdot\exp(-t/T_1)$ where A and B are constants and t is the time after the inversion pulse. Subsequent to slice-selective inversion, fully relaxed blood water proton spins move from outside of the inverted slice into the slice of interest first to the intravascular space and then into the tissue due to exchange. In the macrovasculature where exchange with tissue does not take place, apparent relaxation in the slice-selective IR sequence will be rapid and will depend on flow rate and path length to be traversed in the inversion slice. Beyond this fast macrovascular inflow effect, the slower capillary flow and penetration into tissue due capillary-tissue water exchange and diffusion (i.e., perfusion) should be detected in the presence of sufficient signal-to-noise ratio (SNR). Assuming that the capillary-tissue exchange is fast relative to T_1, relaxation of the longitudinal magnetization in slice selective IR images is described by $M_{ss}(t) = A - B\cdot\exp(-t/T_1^*)$ where T_1^* is the apparent longitudinal relaxation time and $1/T_1^*$ is equal to $1/T_1 + f/\lambda$ where f is the rCBF [ml of blood/(g of tissue·s)] and λ is the tissue-blood partition coefficient [(g of water/g of tissue)/(g of water/ml of blood)] (31). The FAIR image is generated by subtraction $M_{ns}(t)$ from $M_{ss}(t)$; the difference $\Delta M(t)$ is $-B\cdot\exp(-t/T_1)\cdot[1 - \exp(-t\cdot f/\lambda)]$. Because CBF is approximately 0.01 ml/g tissue/s (i.e., 60 ml/100 g of tissue/min) and λ is 0.9 (32), the exponential term can be expanded. Then,

$$\Delta M(t) = B \cdot t \cdot f/\lambda \cdot \exp(-t/T_1). \quad [1]$$

The maximal signal difference will be when $t = T_1$.

In functional activation studies, two IR images are alternately and repeatedly acquired during both control and task periods. Then the differences between each pair of consecutive slice-selective and nonselective IR images are calculated during control periods ($\Delta M_{cont}(t)$) and stimulation periods ($\Delta M_{st}(t)$). Relative signal changes during task periods (ΔS_{FAIR}) can be described as

$$\Delta S_{FAIR} = \Delta M_{st}(t)/\Delta M_{cont}(t) - 1 = rCBF_{st}/rCBF_{cont} - 1 \quad [2]$$

where $rCBF_{st}$ and $rCBF_{cont}$ are the rCBF during task and control periods, respectively. The relative signal change, ΔS_{FAIR}, is the relative blood flow during the task period and independent of t, λ, and T_1.

Due to the use of EPI data collection in this study, it is inevitable to have T_2^* contribution as well as T_1 relaxation in the IR images. The signal intensity of the nonselective IR image at an echo time of TE, $S_{ns}(TE)$, is $M_{ns}(t)\cdot\exp(-TE/T_2^*)$. The difference of signal intensity between selective and global inversion, $\Delta S(TE)$, is

$$\begin{aligned}\Delta S(TE) &= \Delta M(t) \cdot \exp(-TE/T_2^*) \\ &= B \cdot t \cdot f/\lambda \cdot \exp(-t/T_1) \cdot \exp(-TE/T_2^*).\end{aligned} \quad [3]$$

During task periods, both rCBF and $1/T_2^*$ can change. The latter is the source of the BOLD effect. Thus, Eq. [2] must be modified and becomes

$$\begin{aligned}\Delta S_{FAIR}(TE) &= [\Delta S_{st}(TE)/\Delta S_{cont}(TE)] - 1 \\ &= [rCBF_{st}/rCBF_{cont}] \cdot \beta_{BOLD}(TE)] - 1,\end{aligned} \quad [4]$$

where $\Delta S_{st}(TE)$ and $\Delta S_{cont}(TE)$ are FAIR signal intensities during stimulation and control periods, respectively. $\beta_{BOLD}(TE) = \exp(-TE\cdot\Delta(1/T_2^*))$ where $\Delta(1/T_2^*)$ represents the change in $1/T_2^*$ (stimulation minus control). Rewriting Eq. [4], the relative regional cerebral blood flow changes, ΔrelCBF, can be determined by

$$\begin{aligned}\Delta relCBF &= rCBF_{st}/rCBF_{cont} - 1 \\ &= [(\Delta S_{FAIR}(TE) + 1)/\beta_{BOLD}(TE)] - 1.\end{aligned} \quad [5]$$

$\beta_{BOLD}(TE)$ can be directly determined from the consecutive nonselective IR images. Thus, in the FAIR technique, all but the flow effects can be eliminated so that relCBF changes due to tasking can be determined from the FAIR image in a functional imaging protocol provided the "fast exchange" assumption is valid. When the slice-selective IR sequence is used by itself to generate functional map

(3), T_2* BOLD effect is intermixed with the T_1 and flow effects. Similarly, magnetization transfer effect would be minimized in the FAIR image because of the use of a short inversion pulse which is applied in both IR sequences albeit in the presence or absence of slice selective gradients.

MATERIALS AND METHODS

Studies were performed on a 4-T whole body imaging system with a 1.25-m diameter horizontal bore (SIS Co., Sunnyvale, CA/Siemens, Erlangen, Germany) and a head gradient insert with a gradient strength of 30 mT/m and a slew rate of 150 T/m/s in all three axes. For RF transmission and detection, a homogeneous quadrature bird cage coil was used. Manual shimming was performed to improve homogeneity before the image data collection.

The FAIR scheme was implemented with two IR images with and without slice-selective gradients during an inversion pulse in an interleaved fashion. The only difference between these two IR images was the slice-selection gradient during the inversion pulse. All other parameters, including the inversion pulse power, duration, phase and amplitude modulation schemes were kept constant. The inversion pulses were hyperbolic secant pulses with a R value of 10 and a pulse length of 8 ms (33). After an inversion pulse and a subsequent delay, EPI images were acquired with trapezoidal gradient shapes for the readout and blipped gradients for the phase-encoding direction. A single-shot EPI image had a 64×64 matrix size over a field of view of 24×24 cm^2. Total acquisition time was 30 ms. In-plane resolution was 3.8 mm $\times$ 3.8 mm with a 5-mm slice thickness. A five-lobe sinc-shaped RF pulse was used for the excitation to impart a 90° rotation with a pulse length of 4 ms. To demonstrate the effectiveness of the FAIR technique, a stationary phantom containing saline solution was used. Imaging parameters were an inversion time (TI) of 1.4 s, an interimage time of 2.8 s and a inversion slab thickness of 15 mm. Fifty consecutive FAIR images were acquired and then mean and standard deviation of images were calculated.

For functional activation studies, TI of 1.1–1.4 s and an interimage time of 2.5–2.9 s were used. The inversion times were close to T_1 of tissues at 4 T (0.94 and 1.35 s for white and gray matter, respectively) (34), in which maximal signal differences between two IR images were obtained (see Theory). For an imaging slice thickness of 5 mm, a slab thickness of 15–22 mm was inverted for the slice-selective IR images, which corresponds to a distance of 7.5–11 mm from the center and a distance of 5–8.5 mm from the outer edges of the imaging slice. Centers of both imaging and inversion slices were positioned at the same location.

Four normal volunteers were studied according to guidelines by the internal review board of the University of Minnesota; informed consent was obtained from all subjects. Consecutive FAIR EPI images were collected, first under a resting "nonstimulated" state, then during a "task" period, and ending with a "nonstimulated" recovery state. Usually 32 pairs of IR images were acquired in each period. The task was repetitive, sequential finger movements between the thumb and the remaining four digits; three subjects performed unilateral movements, whereas one subject moved bilaterally. The time to start and to stop the movements was indicated by a light-emitting diode placed inside the magnet bore in front of the subject.

From the consecutive FAIR images generated during the paradigm, functional maps were calculated. First, FAIR images were calculated by magnitude subtraction; because we typically collected 32 pairs of IR images, 63 difference images were calculated for each period using 32 intrapair and 31 interpair subtraction images. Student's t tests were performed to compare separately (i) the pre-task control and task periods and (ii) the post-task control and task periods ($P < 0.1$); only pixels with statistically significant activation in both tests were included in the functional map. RelCBF changes using Eq. [5] and time courses were calculated as the average of all activated pixels in the region of interest. Details of the analyses were the same as described elsewhere (10–12).

RESULTS

Phantom experiments were performed with similar imaging parameters (a 5-mm imaging slice with a 15-mm inversion slab) used in functional imaging studies. Signal intensity fluctuations (ΔM) of the FAIR images were 0.98 $\pm$ 0.73 SD % ($n = 50$) of the corresponding nonselective IR images.

Figure 1 shows relCBF measurements of one subject using the FAIR technique during bilateral finger opposition movements. This figure consists of an anatomic image (A), and an IR image (B), a FAIR image (C), a calculated functional map superimposed on these three images (D, E, and F, respectively), and regions of interest (G), from which average time courses (H, I, and J) are presented. A high resolution (256×256) T_1-weighted anatomic image (A) was acquired with a slice-selective inversion pulse and a TI of 1.2 s to have gray/white matter contrast and signal enhancement at vessel areas; it shows large vessel areas with high signal intensity. The slice-selective IR image (B) acquired during functional imaging studies has gray/white matter contrast by itself because an inversion time of 1.1 s was employed. The FAIR image (C) between slice-selective and nonselective IR images provides information of inflow. High signal intensity in the difference images indicates large inflow areas. The signal enhancement due to inflow in the large vessels is high and leads to the white areas in the FAIR image. More importantly, however, smaller changes are present in the diffused tissue areas. To obtain signal intensities, gray and white matter areas were chosen devoid of large vessels (confirmed by the FAIR image). The FAIR intensities of gray and white matter areas (C) were 7.2 and 2.0% of those in the nonselective IR images, which are close to the predicted values of 12.2 and 2.0% calculated using Eq. [1] with f of 0.01 ml/(g of tissue·s) and λ of 0.9.

The ΔrelCBF map during *bilateral* finger opposition movements is overlaid on the high resolution anatomic, IR, and FAIR images (D, E, and F, respectively). The map was not zero-filled or apodized, and consequently indi-

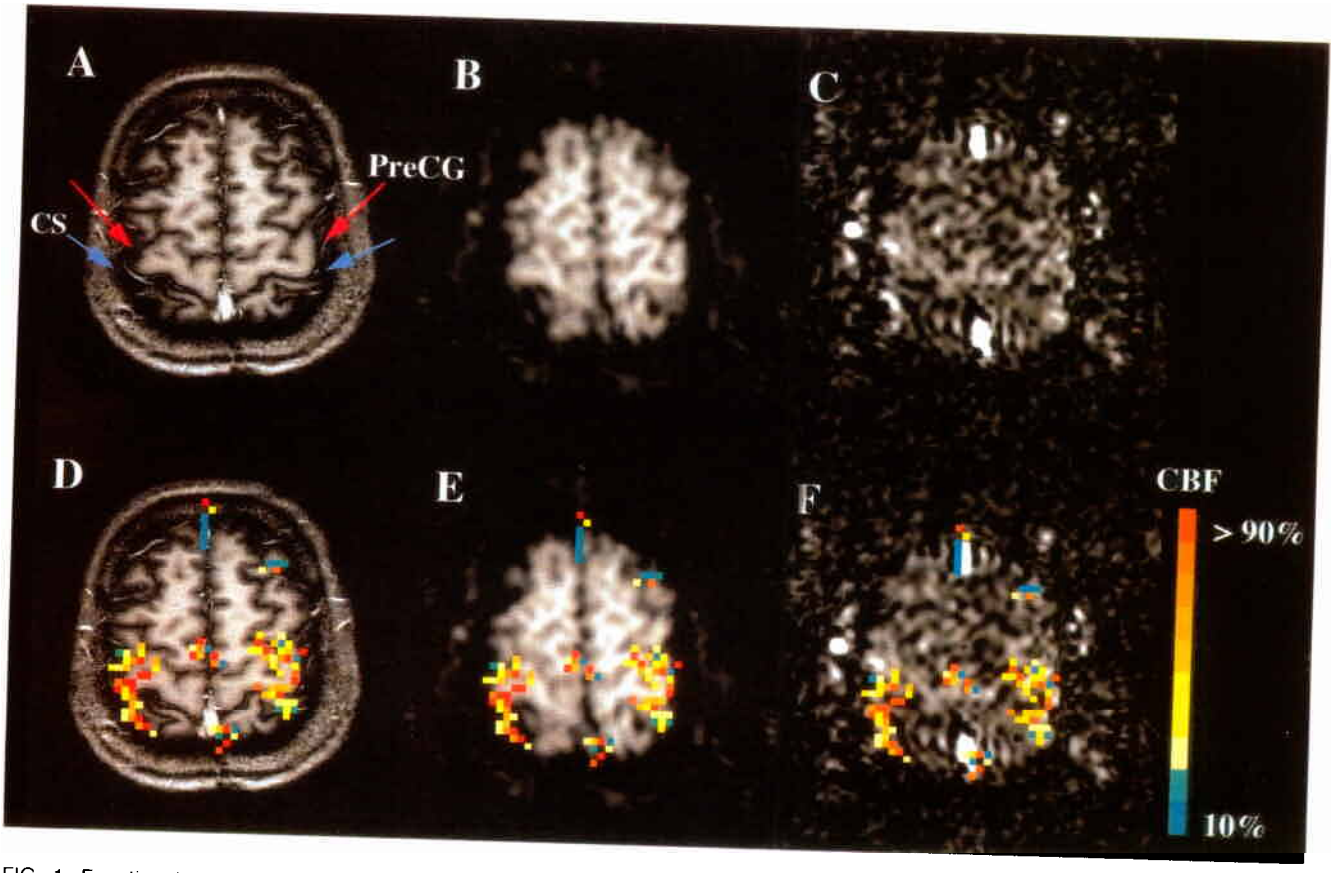

FIG. 1. Functional studies using the FAIR technique during bilateral finger movements. A, B, and C represent a high resolution T_1-weighted (TI = 1.2 s, *TE* = 5 ms, and *TR* = 10 ms) image, a representative slice-selective IR image (TI = 1.1 s, *TE* = 20 ms, *TR* = 2.55 s, and thickness of inversion slab = 22 mm), and a representative FAIR image, respectively. D, E, and F represent the color-coded relCBF change map overlaid on the anatomic, IR, and FAIR images, respectively. Each color in the functional maps represents a 10% increment starting from the bottom (10%). Red and blue arrows indicate the precentral gyrus (PreCG) and central sulcus (CS), top is anterior, and right is the left hemisphere of the subject. G indicates the regions of interest by yellow boxes with the region number for time course analyses shown in H, I, and J, which were averaged from the activated pixels shown in boxes 1, 2, and 3, respectively. Areas 1 and 2 consist of primary motor (posterior side of the precentral gyrus), premotor (anterior side of the precentral gyrus), and somatosensory (posterior side of the central sulcus) areas and area 3 is the supplementary motor area. The left and right time courses in H, I and J came from the same pixels of IR and FAIR (difference) images, respectively. Solid and dotted lines in the left column represent slice-selective and non-slice selective IR image intensities, respectively. Boxes in H, I, and J below time courses indicate task periods.

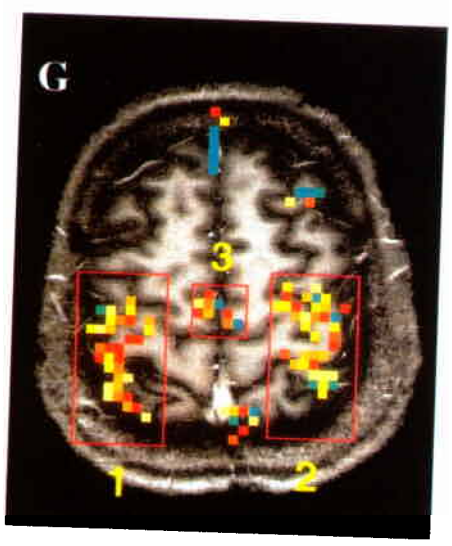

FIG. 1G.

vidual pixels are discernible as small squares at the relatively low resolution of 3.8×3.8 mm^2. Localized activation was observed in motor cortical areas labeled in G, which are the motor cortex (areas 1 and 2; posterior side of the precentral gyrus), premotor (areas 1 and 2; anterior side of the precentral gyrus), supplementary motor (area 3), and somatosensory area due to finger touching in the postcentral gyrus (area 1 and 2; posterior to the central sulcus). These activation sites are consistent with those reported by previous mapping studies based on fMRI and PET during similar movements (10–11, 35–38). The activation areas were predominately at the gray matter area rather than white matter area (see D and E) and located mainly at the diffused tissue areas (F). The average signal changes in the motor areas were between 48 and 68%.

The important feature of the FAIR technique is that macrovascular flow effects and patterns can be easily visualized as very high intensity areas and the FAIR images can be made selectively sensitive to the microvascular effects using long inversion time. As can be

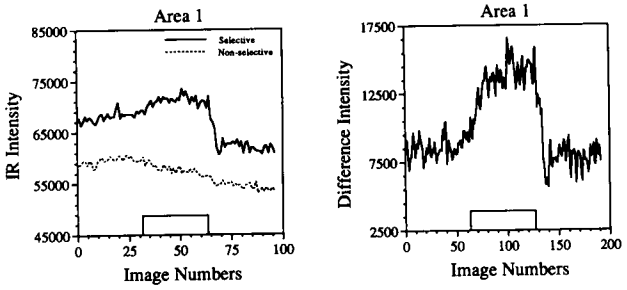

FIG. 1H.

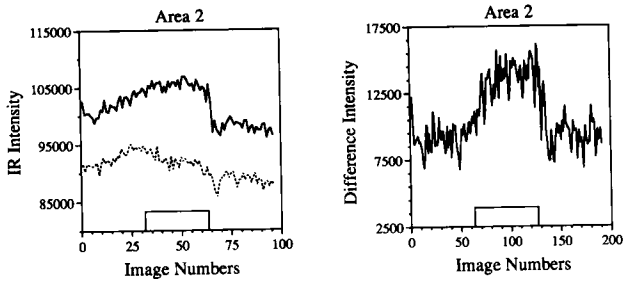

FIG. 1I.

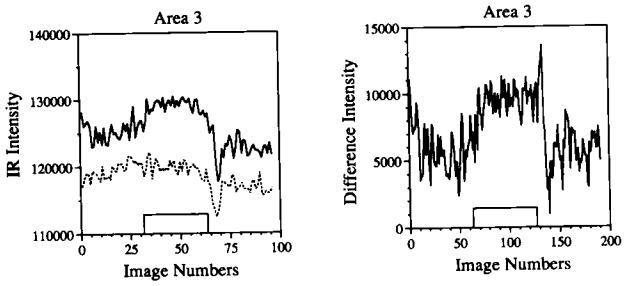

FIG. 1J.

deduced from Figs. 1D and 1F, few pixels were "activated" in areas corresponding to large vessels in the anterior and posterior of the head, which are the sagittal sinus. Unlike BOLD images, however, these pixels show very small task-related relative signal change whereas tissue areas devoid of large vessels yield the largest signal changes with the FAIR technique. These small, task-induced macrovascular effects can be further suppressed and microvascular component enhanced further by going to longer TI values (see below).

To compare the FAIR method and the slice-selective IR method, time courses of FAIR (right column) and IR (left column; solid and dashed lines for slice-selective and non-slice-selective IR) images are shown in Figs. 1H, 1I, and 1J. Relative signal intensities were averaged from activated pixels in marked areas in Fig. 1G. Clearly, there is global signal drifting in areas 1, 2, and 3 possibly due to motion and T_2* change. The percent signal changes in the IR images (left time courses) were small and are also sensitive to baseline drifts. However, relative signal changes in the FAIR images (right time courses) were much greater although absolute signal changes may be the same. Furthermore, because the FAIR images can subtract out signal fluctuations contained in both slice-selective and nonselective IR images, flat baselines are observed during the two control periods, before and after the stimulation period, improving effective contrast-to-noise. This is demonstrated especially in area 2, where signal changes cannot be easily determined from IR images alone because of the baseline drift, whereas the relCBF change can be easily calculated from the FAIR images.

Figure 2 shows a functional activation ΔrelCBF map of a different subject during *unilateral* finger movements. The left motor cortex was activated during right hand finger movements, which is consistent with previous studies (10–11, 35–38). Additional activation was seen in the somatosensory area in the post-central gyrus due to touching of fingers, and contralateral premotor areas, all as expected. Also it should be noted that macrovascular effects were eliminated in this image with the uses of longer (1.4 s) inversion time and thinner (15 mm) inversion slab (see below). Average signal changes in the left motor cortex, ipsilateral premotor and supplementary motor areas were 30, 29, and 23%, respectively.

The FAIR signal intensities (ΔM_{cont} and ΔM_{st}) of contralateral motor cortical area (average of all "activated pixels") in four subjects during control and task periods were 13.8 ± 8.8 and 19.8 ± 11.1% SD of those in the corresponding nonselective IR images (n = 5 because one subject performed bilateral movements and both motor cortical areas were included separately), respectively. The signal change (ΔS_{FAIR}) of contralateral motor cortical area detected by the FAIR technique was 48 ± 14% SD (n = 5) and ranged between 30 and 68%, which is in good agreement with PET studies of blood flow (35–38).

DISCUSSION

We have developed a novel FAIR-based perfusion imaging technique to measure relative cerebral blood flow changes and applied it to measure relCBF changes of the human brain during finger movements. This relCBF measurement is similar to the relCBF measurement technique by PET. The PET technique involves injection of $H_2{}^{15}O$ tracer and count of positron emission separately for two different experimental conditions; one during control and the other during task periods. Then, the ratio of positron count is calculated on a pixel-by-pixel basis, which is the relative blood flow. Although the FAIR technique provides the same relCBF information compared to PET, the MR method provides advantages due to availability of higher resolution, ease of use and absence of any invasive procedures. The imaging time of the FAIR technique can also be shorter than that of PET relCBF measurements, which need an inter-experiment delay due to the half-life of ^{15}O (123 s), in addition to data acquisition.

During the finger movements, the relCBF changes in the motor area studied by PET and xenon-133 were between 20 and 40%; 40% by Roland *et al.* (35), 30% by Seitz and Roland (36), 36% by Grafton *et al.* (37), and 20% by Colebatch *et al.* (38). Typical resolution of these radioisotope methods was 10 × 10 × 10 mm^3. Considering the relatively high resolution of the voxel in this study (3.8 × 3.8 × 5 mm^3), relatively higher relCBF

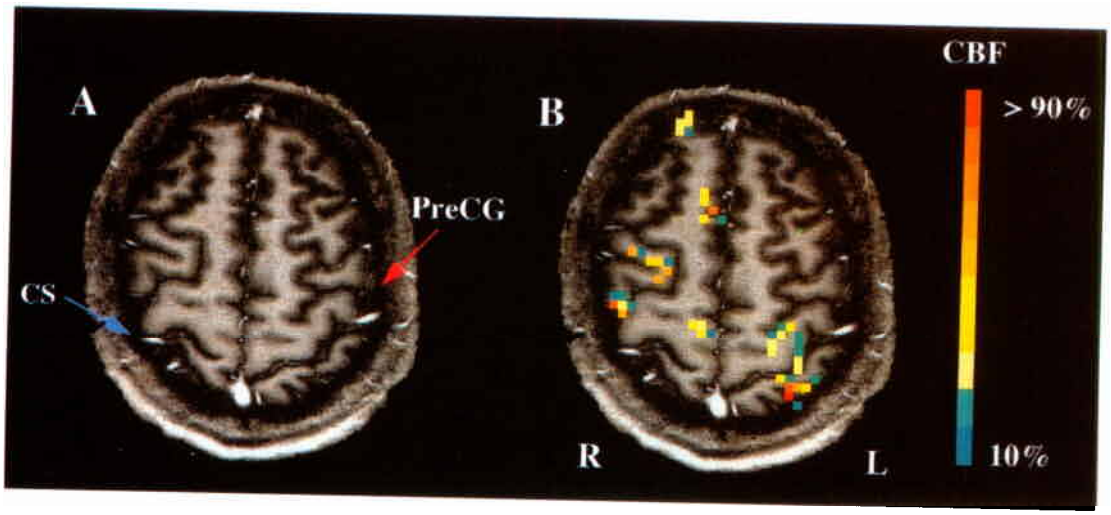

FIG. 2. High resolution anatomic image (A) and color-coded functional map overlaid on the anatomic image (B) during right finger movements. For the FAIR technique, the following parameters were used; TI = 1.4 s, *TE* = 20 ms, *TR* = 2.85 s, and thickness of inversion slab = 15 mm. Each color in the functional maps represents a 10% increment starting from the bottom (10%). The left motor cortex was activated during tasks. A red arrow indicates the precentral gyrus (PreCG), the blue arrow represents the central sulcus (CS), top is anterior, and right is the left hemisphere (L) of the subject.

changes can be expected because of reduced partial volume effects. Generally the relCBF values measured by the FAIR technique (30–68%) in this preliminary study agree well with those reported from PET and xenon-133 studies.

One of the important issues in the fMRI studies is the contribution of large vessels. In the FAIR technique, the flow velocity v and the thickness of a slice-selective inversion slab (i.e., travel distance of blood spins, D) are the critical components of the vessel contributions. The degree, to which spins in the imaging slice are refreshed has a straightforward dependence on v, TI, and D. Complete refreshment occurs when $v \geq D/\mathrm{TI}$. For example, an inversion slab of 15–22 mm with an imaging slice thickness of 5 mm means that a travel distance (D) of blood from the inferior end of inversion slab to the superior end of the imaging slice is 10–13.5 mm. Because the arteries have flow velocities of >5 cm/s (39), fresh blood spins will be completely replenished during the inversion time of 1.1–1.4 s, regardless of control or stimulation periods. Thus, increases of these flows do not induce significant signal changes. But arterioles have blood velocity of 1 cm/s (39), and thus blood in arterioles will travel 11–14 mm during TI of 1.1–1.4 s, which can be less than D. Thus, there may be signal changes in the arterioles due to flow changes during task periods. To further reduce the macrovasculature contributions in the functional images, the travel distance of arterial blood can be shortened by a thinner inversion slab and/or a longer inversion time, both of which is possible and remains to be explored.

A BOLD-based technique is most widely used in fMRI studies. The BOLD phenomenon has two components (24); one is due to dephasing of the magnetization in the presence of susceptibility-induced gradients of relatively large venous vessels, and the other is due to diffusion within the steep, susceptibility-induced gradients from small vessels (capillaries and venules). These suggest the BOLD changes are small and may be predominantly at large venous vessels at low magnetic fields (40–45). Contrary to BOLD effects, relCBF changes will be, in theory, the same whether measurements are performed on high or low field systems. Therefore, relCBF measurements using the FAIR technique can be performed even at low magnetic fields provided adequate SNR can be achieved. The main differences are that high fields provide a higher SNR and a longer T_1 of tissue water which is advantageous for differentiating macrovascular flow from microvascular flow and perfusion. The disadvantages of the FAIR technique are a poor temporal resolution and a long acquisition time required for whole brain mapping compared to the BOLD-based technique. Using both the FAIR and BOLD techniques will enhance understanding of brain function. Because BOLD effects can be determined by nonselective IR images and relCBF from the FAIR images, both relCBF and BOLD changes are present in the FAIR technique.

In the functional MRI studies, baseline drift is a problem because functional maps are calculated from comparison between control and task-induced signal intensities. This drift may be due to physiological changes induced by effects such as anxiety and anticipation, subject's motion (even if sub-pixel movements) (46), and approach to steady-state magnetization if relatively fast repetition of RF pulses is employed. Slight, not abrupt, baseline changes can be corrected by subtraction of an image from its neighbor image. We demonstrated the effectiveness of removal of baseline drift in time courses of FAIR images (Fig. 1).

Several assumptions have been made to determine relCBF changes from the FAIR technique. (i) It has been assumed that there is rapid equilibrium of water concentration between the vascular and extravascular spaces of the brain. Using labeled water ^2H_2O and $H_2{}^{15}O$, many attempts have been made to validate that water is a freely diffusible tracer (47–52). Although this assumption may

not be true in the brain at high blood flow rates (47–48), the use of water as a perfusion tracer is valid at the flow rate of <250 ml/(100 g·min) (52). Given the average intercapillary distance of 25 μm in brain (53), the relevant diffusion distance is 12.5 μm. Using the equation $r^2 = 6Dt$ where r is the displacement, D is the diffusion coefficient, and t is the diffusion time, an estimated diffusion time is approximately 24 ms based on the experimentally determined diffusion constant of 1.1×10^{-5} cm^2/s in the human brain (54). Therefore, given our inversion time, fast exchange conditions would be satisfied provided that the capillary-tissue exchange rate is also rapid relative to T_1. Although there are no rigorous data on this, calculations based on this assumption yield accurate results for CBF (52, 55). (ii) We assumed that the feeding flow direction is perpendicular to the imaging plane. In cases where the flow travels parallel to the imaging slice *during whole inversion time*, signal enhancements in the FAIR images cannot be detected. Thus, slice position and orientation should be chosen carefully. (iii) We have made the assumption that there is no flow component in the nonselective IR images. Although a homogeneous coil was used in this study, the images may have flow contributions from large arteries with fast flow rates. This problem can be eliminated by using a body coil for RF excitation. In functional imaging studies, this may not be a problem because blood flow in the major feeding arteries may not be altered during task periods (23, 56). (iv) The inversion slab is assumed to have the same thickness as the imaging slice. In practice, the inversion slab is chosen to be thicker than the imaging slab to eliminate effects from the imperfect edges of the inversion pulse. Spins outside the imaging slice but inside the inverted slab do not directly contribute flow effects in the slice-selective IR images (as in nonselective inversion). This makes the travel distance of fresh spins longer, creating potential errors in the quantitation of flow. Thus, blood flow derived from the FAIR technique may originate from the average inversion slab rather than the imaging slice. The relationship between slab thickness and rCBF needs to be further investigated (see above). (v) Eqs. [1]–[5] are based on the full relaxation of magnetization. The exact relationship between signal change under the steady state condition and relCBF needs to be studied.

CONCLUSION

We have developed a new perfusion imaging technique based on IR images and subtraction, which is called FAIR. This FAIR technique has been successfully applied to human brain functional studies and used to measure the relative blood flow changes during tasking. Unlike that seen in the BOLD effect, the cerebral blood flow change is expected to be relatively independent of the magnetic field strength. With the proper inversion time and thickness of inversion slab, only microvascular-based functional maps can be obtained. The image acquired with the FAIR technique provides anatomic and vessel information.

ACKNOWLEDGMENTS

The author thanks Drs. Kamil Ugurbil, Xiaoping Hu, and Wei Chen for stimulating discussions, Dr. Peter Andersen for hardware support and proof-reading, Tuong Le for help in data processing, Gregor Adriany for a quadrature bird cage coil, and John Strupp for his processing software (STIMULATE).

REFERENCES

1. M. E. Raichle, Circulatory and metabolic correlates of brain functional in normal humans. *Handb. Physiol.* **5,** 643–674 (1987).
2. S. Ogawa, D. W. Tank, R. S. Menon, J. M. Ellermann, S.-G. Kim, H. Merkle, K. Ugurbil, Intrinsic signal changes accompanying sensory stimulation: functional brain mapping using MRI. *Proc. Natl. Acad. Sci. (USA)* **89,** 5951–5955 (1992).
3. K. K. Kwong, J. W. Belliveau, D. A. Chesler, I. E. Goldberg, R. M. Weisskoff, B. P. Poncelet, D. N. Kennedy, B. E. Hoppel, M. S. Cohen, R. Turner, H.-M. Cheng, T. J. Brady, B. R. Rosen, Dynamic magnetic resonance imaging of human brain activity during primary sensory stimulation. *Proc. Natl. Acad. Sci. (USA)* **89,** 5675–5679 (1992).
4. P. A. Bandettini, E. C. Wong, R. S. Hinks, R. S. Tikofsky, and J. S. Hyde, Time course EPI of human brain function during task activation. *Magn. Reson. Med.* **25,** 390–397 (1992).
5. K. R. Thulborn, J. C. Waterton, P. M. Mattews, G. K. Radda, Oxygenation dependence of the transverse relaxation time of water protons in whole blood at high field. *Biochim. Biophys. Acta* **714,** 265–270 (1982).
6. S. Ogawa, T.-M. Lee, A. S. Nayak, P. Glynn, Oxygenation-sensitive contrast in magnetic resonance imaging of rodent brain at high magnetic fields. *Magn. Reson. Med.* **14,** 68–78 (1990).
7. S. Ogawa, T.-M. Lee, A. R. Kay, D. W. Tank, Brain magnetic resonance imaging with contrast dependent on blood oxygenation. *Proc. Natl. Acad. Sci. (USA)* **87,** 9868–9872 (1990).
8. S. Ogawa, T.-M. Lee, Magnetic resonance imaging of blood vessels at high fields: *in vivo* and *in vitro* measurements and image simulation. *Magn. Reson. Med.* **16,** 9–18 (1990)
9. P. T. Fox, M. E. Raichle, Focal physiological uncoupling of cerebral blood flow and oxidative metabolism during somatosensory stimulation in human subjects. *Proc. Natl. Acad. Sci. (USA)* **83,** 1140–1144 (1986).
10. S.-G. Kim, J. Ashe, A. Georgopoulos, H. Merkle, J. M. Ellermann, R. S. Menon, S. Ogawa, K. Ugurbil, Functional imaging of human motor cortex at high magnetic field. *J. Neurophysiol.* **69,** 297–302 (1993).
11. S.-G. Kim, J. Ashe, K. Hendrich, J. M. Ellermann, H. Merkle, K. Ugurbil, A. Georgopoulos, Functional magnetic resonance imaging of motor cortex: hemispheric asymmetry and handedness. *Science* **261,** 615–617 (1993).
12. S.-G. Kim, K. Ugurbil, P. L. Strick, Activation of a cerebellar output nucleus during cognitive processing. *Science* **265,** 949–951 (1994).
13. R. Turner, P. Jezzard, H. Wen, K. K. Kwong, D. Le Bihan, T. Zeffiro, R. Balaban, Functional mapping of the human visual cortex at 4 and 1.5 Tesla using deoxygenation contrast EPI. *Magn. Reson. Med.* **29,** 277–279 (1993).
14. A. M. Blamire, S. Ogawa, K. Ugurbil, D. Rothman, G. McCarthy, J. Ellermann, F. Hyder, Z. Rattner, R. G. Shulman, Dynamic mapping of the human visual cortex by high-speed magnetic resonance imaging. *Proc. Natl. Acad. Sci. (USA)* **89,** 11069–11073 (1992).
15. J. Frahm, K. D. Merboldt, W. Hanicke, Functional MRI of

human brain activation at high spatial resolution. *Magn. Reson. Med.* **29,** 139–144 (1993).
16. R. M. Hinke, X. Hu, A. E. Stillman, S.-G. Kim, H. Merkle, R. Salmi, K. Ugurbil, Functional magnetic resonance imaging of Broca's area during internal speech. *NeuroReport* **4,** 675–678 (1993).
17. R. T. Constable, G. McCarthy, T. Allison, A. W. Snderson, J. R. Gore, Functional brain imaging at 1.5 Tesla using conventional gradient echo imaging techniques. *Magn. Reson. Imaging* **11,** 451–459 (1993).
18. D. Le Bihan, R. Turner, T. A. Zeffiro, C. A. Cuenod, P. Jezzard, V. Bonnerot, Activation of human primary visual cortex during visual recall: a magnetic resonance imaging study. *Proc. Natl. Acad. Sci. (USA)* **90,** 11802–11805 (1993).
19. G. McCarthy, A. M. Blamire, D. G. Rothman, R. Gruetter, R. G. Shulman, Echo-planar magnetic resonance imaging studies of frontal cortex activation during word generation in humans. *Proc. Natl. Acad. Sci. (USA)* **90,** 4952–4956 (1993).
20. A. Connelly, G. D. Jackson, R. S. J. Frankowiak, J. W. Belliveau, F. Vargha-Khadem, D. G. Gadian, Functional mapping of activated human primary cortex with a clinical MR imaging system. *Radiology* **188,** 125–130 (1993).
21. W. Schneider, D. G. Noll, J. G. Cohen, Functional topographic mapping of the cortical ribbon in human vision with conventional MRI scanners. *Nature* **365,** 150–153 (1993).
22. P. E. Roland, L. Eriksson, S. Stone-Elander, L. Widen, Does mental activity change the oxidative metabolism of the brain? *J. Neurosci.* **7,** 2373–2389 (1987).
23. R. J. Seitz, P. E. Roland, Vibratory stimulation increases and decreases the regional cerebral blood flow and oxidative metabolism: a positron emission tomography (PET) study. *Acta Neurol. Scand.* **86,** 60–67 (1992).
24. S. Ogawa, R. S. Menon, D. W. Tank, S.-G. Kim, H. Merkle, J. M. Ellermann, K. Ugurbil, Functional brain mapping by blood oxygenation level-dependent contrast magnetic resonance imaging. *Biophys. J.* **64,** 803–812 (1993).
25. S. Ogawa, T. M. Lee, B. Barrere, The sensitivity of magnetic resonance imaging signals of a rat brain to changes in the cerebral venous blood oxygenation. *Magn. Reson. Med.* **29,** 205–210 (1993).
26. F. Prielmeier, Y. Nagatomo, J. Frahm, Cerebral blood oxygenation in rat brain during hypoxic hypoxia. Quantitative MRI of effective transverse relaxation rates. *Magn. Reson. Med.* **31,** 678–681 (1994).
27. J. W. Belliveau, D. N. Kennedy, R. C. McKinstry, B. R. Buchbinder, R. M. Weisskoff, M. S. Cohen, J. M. Vevea, T. J. Brady, B. R. Rosen, Functional mapping of the human visual cortex by magnetic resonance imaging. *Science* **254,** 716–719 (1991).
28. K. K. Kwong, D. A. Chesler, C. S. Zuo, J. L. Boxerman, J. R. Baker, Y. C. Chen, C. S. Stern, R. M. Weisskoff, B. R. Rosen, Spin echo (T_2, T_1) studies for functional MRI, *in* "Proc., Society of Magnetic Resonance, 1993," p. 172.
29. K. K. Kwong, D. A. Chesler, R. M. Weisskoff, B. R. Rosen, Perfusion MR imaging, *in* "Proc., Society of Magnetic Resonance, 1994," p. 1005.
30. R. E. Edelman, B. Siewert, D. G. Darby, V. Thangaraj, A. C. Nobre, M. M. Mesulam, S. Warach, Qualitative mapping of cerebral blood flow and functional localization with echo-planar MR imaging and signal targeting with alternating radio frequency. *Radiology* **192,** 513–520 (1994).
31. J. A. Detre, J. S. Leigh, D. S. Williams, A. P. Koretsky, Perfusion imaging. *Magn. Reson. Med.* **23,** 37–45 (1992).
32. P. Herscovitch, M. E. Raichle, What is the correct value for the brain-blood partition coefficient for water? *J Cereb. Blood Flow Metab.* **5,** 65–69 (1985).
33. M. Garwood, K. Ugurbil, B_1 Insensitive adiabatic pulses. *NMR Basic Principles and Progress* **26,** 110–147 (1992).
34. S.-G. Kim, X. Hu, K. Ugurbil, Accurate T_1 determination from inversion recovery images: application to human brain at 4 Tesla. *Magn. Reson. Med.* **31,** 445–449 (1994).
35. P. E. Roland, B. Larsen, N. A. Larsen, E. Skinoj, Supplementary motor area and other cortical areas in organization of voluntary movements in man. *J. Neurophysiol.* **43,** 118–136 (1980).
36. D. J. Seitz, P. E. Roland, Learning of sequential finger movements in man: a combined kinematic and positron emission tomography (PET) study. *Eur. J. Neurosci.* **4,** 154–165 (1992).
37. S. T. Grafton, R. P. Woods, J. C. Mazziotta, M. E. Phelps, Somatotopic mapping of the primary motor cortex: activation studies with cerebral blood flow and positron emission tomography. *J. Neurophysiol.* **66,** 735–743 (1991).
38. J. G. Colebatch, M.-P. Deiber, R. E. Passingham, K. J. Friston, R. S. J. Frackowiak, Regional cerebral blood flow during voluntary arm and hand movements in human subjects. *J. Neurophysiol.* **65,** 1392–1401 (1991).
39. H. van As, T. J. Schaaffsma, Flow in nuclear magnetic resonance imaging, *in* "Introduction to Biomedical Nuclear Resonance" (S. B. Petersen, R. N. Muller, P.A. Rinck, Eds.), Ch. 11, pp. 68–95, Georg Theme Verlag, New York, 1985.
40. R. S. Menon, S. Ogawa, D. W. Tank, K. Ugurbil, 4 Tesla gradient recalled echo characteristic of photic stimulation-induced signal changes in the human primary visual cortex. *Magn. Reson. Med.* **30,** 380–386 (1993).
41. S. Lai, A. L. Hopkins, E. M. Haacke, D. Li, B. A. Wasserman, P. Buckley, L. Friedman, H. Meltzer, P. Hedera, R. Friedland, Identification of vascular structures as a major source of signal contrast in high resolution 2D and 3D functional activation imaging of the motor cortex at 1.5 T: preliminary results. *Magn. Reson. Med.* **30,** 387–392 (1993).
42. S.-G. Kim, K. Hendrich, X. Hu, H. Merkle, K. Ugurbil, Potential pitfalls of functional MRI using conventional gradient-recalled echo techniques. *NMR Biomed.* **7,** 69–74 (1994).
43. J. H. Duyn, C. T. W. Moonen, G. H. van Yperen, R. W. de Boer, P. R. Luyten, Inflow versus deoxyhemoglobin effects in BOLD functional MRI using gradient echoes at 1.5T. *NMR Biomed.* **7,** 4–9 (1994).
44. J. Frahm, K.-D. Merboldt, W. Hanicke, A. Kleinschmidt, H. Boecker, Brain and vein—oxygenation or flow? On signal physiology in functional MRI of human brain activation. *NMR Biomed.* **7,** 45–53 (1994).
45. S. Segebarth, V. Belle, C. Delon, R. Massarelli, J. Decety, J.-F. Le Bas, M. Decorps, A. L. Benabid, Functional MRI of the human brain: predominance of signals from extracerebral veins. *NeuroReport* **5,** 813–816 (1994).
46. J. V. Hajnal, R. Myers, A. Oatridge, J. E. Schwieso, I. R. Young, G. M. Bydder, Artifacts due to stimulus correlated motion in functional imaging of the brain. *Magn. Reson. Med.* **31,** 283–291 (1994).
47. J. O. Eichling, M. E. Raichle, R. L. Grubb, Jr., M. M. Ter-Pogossian, Evidence of the limitations of water as a freely diffusible tracer in brain of the Rhesus monkey. *Circ. Res.* **35,** 358–364 (1974).
48. M. E. Raichle, W. R. W. Martin, P. Hersccovitch, M. A. Mintun, J. Markham, Brain blood flow measured with intravenous $H_2{}^{15}O$. *II. Implementation and validation. J. Nucl. Med.* **24,** 790–798 (1983).
49. J. J. H. Ackerman, C. S. Ewy, N. N. Becker, R. A. Shalwitz, Deuterium nuclear magnetic resonance measurements of blood flow and tissue perfusion employing ^2H_2O as a freely diffusible tracer. *Proc. Natl. Acad. Sci. (USA)* **85,** 4099–4102 (1987).
50. S.-G. Kim, J. J. H. Ackerman, Quantitation of regional blood

flow by monitoring of exogenous tracer via nuclear magnetic resonance spectroscopy. *Magn. Reson. Med.* **14,** 266–282 (1990).
51. J. J. Neil, The validation of freely diffusible tracer methods with NMR detection for measurement of blood flow. *Magn. Reson. Med.* **19,** 299–304 (1991).
52. R. J. T. Corbett, A. P. Laptook, E. Olivares, Simultaneous measurement of cerebral blood flow and energy metabolites in piglets using deuterium and phosphorus nuclear magnetic resonance. *J. Cereb. Blood Flow Metab.* **11,** 55–65 (1991).
53. G. Pawlik, A. Rackl, R. J. Bing, Quantitative capillary topography and blood flow in the cerebral cortex of cats: an in vivo microscopic study. *Brain Res.* **208,** 35–58 (1981).
54. T. L. Chenevert, J. G. Pipe, D. G. Williams, J. A. Brunberg, Quantitative measurement of tissue perfusion and diffusion *in vivo*. *Magn. Reson. Med.* **17,** 197–212 (1991).
55. D. S. Williams, J. A. Detre, J. S. Leigh, A. P. Koresky, Magnetic resonance imaging of perfusion using spin inversion of arterial water. *Proc. Natl. Acad. Sci. (USA)* **89,** 212–216 (1992).
56. L. Sokoloff, R. Mangold, R. L. Wechsler, C. Kennedy and S. Kety, The effect of mental activity on cerebral circulation and metabolism. *J. Clin. Invest.* **34,** 1101–1108 (1955).